

---

Article

Not peer-reviewed version

---

# Experimental Investigation on the Effect of Heating Oil and TPO Combustion on Different Stoichiometric Ratios, Flame Penetration, Emission Characteristics, and Soot Formation in an Evaporative Combustion Chamber

---

István Péter Kondor \*

Posted Date: 27 November 2023

doi: 10.20944/preprints202311.1675.v1

Keywords: heating oil; TPO; steam injection; evaporative combustion chamber



Preprints.org is a free multidiscipline platform providing preprint service that is dedicated to making early versions of research outputs permanently available and citable. Preprints posted at Preprints.org appear in Web of Science, Crossref, Google Scholar, Scilit, Europe PMC.

Copyright: This is an open access article distributed under the Creative Commons Attribution License which permits unrestricted use, distribution, and reproduction in any medium, provided the original work is properly cited.

Disclaimer/Publisher's Note: The statements, opinions, and data contained in all publications are solely those of the individual author(s) and contributor(s) and not of MDPI and/or the editor(s). MDPI and/or the editor(s) disclaim responsibility for any injury to people or property resulting from any ideas, methods, instructions, or products referred to in the content.

## Article

# Experimental Investigation on the Effect of Heating Oil and TPO Combustion on Different Stoichiometric Ratios, Flame Penetration, Emission Characteristics, and Soot Formation in an Evaporative Combustion Chamber

István Péter Kondor

John von Neumann University, 6000 Kecskemét, Hungary; kondor.peter@nje.hu

**Abstract:** This research aims to delve into the intricacies of combustion processes, specifically focusing on heating oil and a blend of heating oil with TPO (Tire Pyrolysis Oil) in a self-developed evaporative combustion chamber featuring steam injection. The primary objective is to scrutinize the impact of steam injection on the combustion dynamics. Conducting a series of tests, the investigation involved the meticulous manipulation of stoichiometric ratios while introducing ambient air through gravity fuel flow. Subsequent iterations of these tests incorporated the introduction of steam into the ambient air stream. The examination encompassed the combustion of both heating oil and the TPO blend within the combustion chamber. The evaluation criteria comprised an in-depth analysis of flame characteristics, temperature distribution within the combustion chamber, and the quantification of emissions such as particulate matter (PM), nitrogen oxides (NO<sub>x</sub>), carbon dioxide (CO<sub>2</sub>), carbon monoxide (CO), and water vapor (H<sub>2</sub>O). Throughout the experimentation phase, commercially available diesel fuel served as the primary fuel source. To facilitate the tests, the combustion chamber under scrutiny was seamlessly integrated into an AVL engine test bench system. Essential parameters, including fuel consumption, were meticulously gauged using an AVL 735 fuel flow meter, while fuel temperature was monitored using the AVL 745 fuel temperature conditioning system. The intake air, a crucial element in the combustion process, was quantified with precision using an AVL Flowsonix sensor. Emission measurements were conducted meticulously using state-of-the-art equipment, with gaseous emissions analyzed using an AVL FTIR AMA i60 exhaust gas analyzer. Simultaneously, soot emissions were quantified through employment of an AVL Micro Soot sensor. This comprehensive approach not only delves into the fundamental aspects of combustion but also extends its reach to the exploration of innovative techniques, such as steam injection, to enhance combustion efficiency and reduce emissions. The integration of advanced measurement tools ensures a robust and thorough analysis of the combustion process and its environmental implications.

**Keywords:** heating oil; TPO; steam injection; evaporative combustion chamber

---

## 1. Introduction

In the contemporary context, the European Union finds itself grappling with the repercussions of the energy crisis and the geopolitical tensions arising from the war in Ukraine, both of which have synergistically propelled the cost of natural gas to unprecedented heights within its borders. The focus has shifted from mere economic considerations of gas prices to a critical concern about the very availability of this vital energy resource in the near future. In response to this looming crisis, the EU has implemented legislation mandating a substantial reduction in gas consumption, compelling a shift toward alternative energy sources to meet heating demands, particularly in the realm of residential and industrial applications [1,2,3]. As a viable substitute for natural gas, various forms of oil—whether fossil, bio, or synthetic—have emerged as focal points in the quest for energy diversification. Fossil oils, exemplified by readily available heating oil with properties akin to diesel fuel, have historically played a role in industrial and power plant settings, and until recently, were

commonly used for household heating. However, the ascendancy of natural gas, owing to its cost-effectiveness and convenience, has relegated heating oil to a secondary position [4]. In the pursuit of mitigating emissions and enhancing the efficiency of oil-based energy systems, steam injection has emerged as a noteworthy technique. Extensive literature research has revealed its application, primarily in internal combustion diesel engines, as a means to alter the dynamics of the combustion process. Armas et al. observed a faster combustion process, decreased combustion temperature, and reduced concentrations of  $\text{NO}_x$ ,  $\text{HC}$ , and particulate matter (PM) through steam injection [5]. Further studies by Kökküünk et al. demonstrated that simulation results aligned closely with experimental data, showcasing an increase in engine torque and effective power by up to 2.5%, along with significant reductions in  $\text{NO}_x$  and  $\text{CO}_2$  emissions [6]. Additional insights from Lin and Wang highlighted the multifaceted impacts of steam injection, including decreased exhaust temperature, lowered levels of  $\text{O}_2$ ,  $\text{NO}_x$ , and smoke, alongside increased  $\text{CO}_2$  and  $\text{CO}$  emissions [7]. It's noteworthy that much of the existing research primarily delves into the intricacies of processes occurring within internal combustion engines. This collective body of knowledge underscores the urgency and complexity of the current energy landscape, necessitating innovative solutions and alternative technologies to navigate the challenges posed by the escalating costs and diminishing availability of natural gas in the European Union.

This research delves into the examination of a uniquely designed evaporative combustion chamber tailored for the combustion of liquid fuels. Within evaporative combustion chambers, the interplay between gravity and ambient pressure air significantly influences the behavior of the liquid fuel during the combustion process. The cylindrical configuration of the combustion chamber incorporates circular vertical pipes strategically designed to enhance heat release. To optimize the combustion efficiency, a thoughtful air supply mechanism has been implemented. Ambient air is introduced into the lower part of the combustion chamber through meticulously drilled circular holes, ensuring a thorough and efficient mixing of air with the liquid fuel. Gravity facilitates the downward flow of the liquid fuel from the fuel tank, filling the bottom of the combustion chamber. Notably, the bottom of the combustion chamber exhibits a dual-layered structure. On the outer part, ambient air is directed into the chamber, complementing the combustion process. Simultaneously, the inner tray at the bottom facilitates the controlled intake of liquid fuel. The inner tray is designed with small circular holes on the side, allowing air to ingress into the combustion zone, further optimizing the combustion reaction. Figure 1 illustrates a detailed 3D model of the combustion chamber, showcasing its cylindrical form with integrated circular vertical pipes and the intricate arrangement of components. The construction material chosen for the combustion chamber is a hot-rolled alloy steel plate, specifically A572GR.50, interconnected through a welding process. This choice of material ensures robustness and durability, crucial for withstanding the harsh conditions associated with combustion processes. In summary, this study not only investigates the functionality of the evaporative combustion chamber but also emphasizes the importance of design elements such as the cylindrical structure, circular pipes, and dual-layered bottom for effective heat release and combustion efficiency. The use of A572GR.50 alloy steel as the construction material further underscores the commitment to durability and reliability in the performance of the combustion chamber.

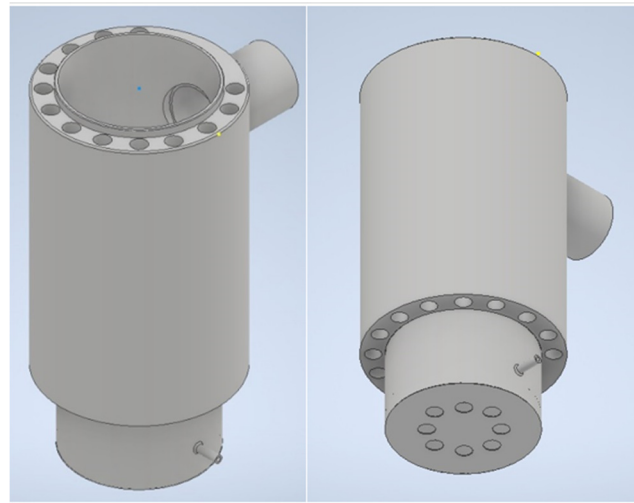


**Figure 1.** Combustion chamber 3D model.

The measurement system employed in this study is seamlessly integrated with a standard AVL engine brake system. The entire process involves the precise control and monitoring of fuel flow, with fuel originating from the fuel tank and passing through a series of components, including a flow meter, conditioner, and pressure regulator, before entering the combustion chamber. The regulator allows for meticulous adjustment of the fuel flow, ensuring optimal conditions for combustion. Simultaneously, the combustion chamber draws in the necessary air from the surrounding environment. This incoming air is directed through a flow meter, and its volume can be finely tuned using a dedicated valve. This dual-control mechanism—fuel flow and air intake—facilitates a comprehensive exploration of combustion dynamics. To assess the environmental impact of the combustion process, the concentration of harmful substances is meticulously analyzed. Exhaust gases emanating from the combustion chamber are sampled for this purpose. The Micro Soot Sensor (MSS) system is employed to measure the amount of soot content, providing insights into particulate matter. Additionally, the gas concentrations are determined using Fourier-Transform Infrared Spectroscopy (FTIR) equipment, allowing for a detailed analysis of various gas components. For a visual representation of the experimental setup, refer to Figure 2, which depicts the schematic diagram of the entire system. This comprehensive setup ensures accurate and controlled measurements, laying the foundation for a thorough investigation into combustion characteristics and emissions in the context of the AVL engine brake system.

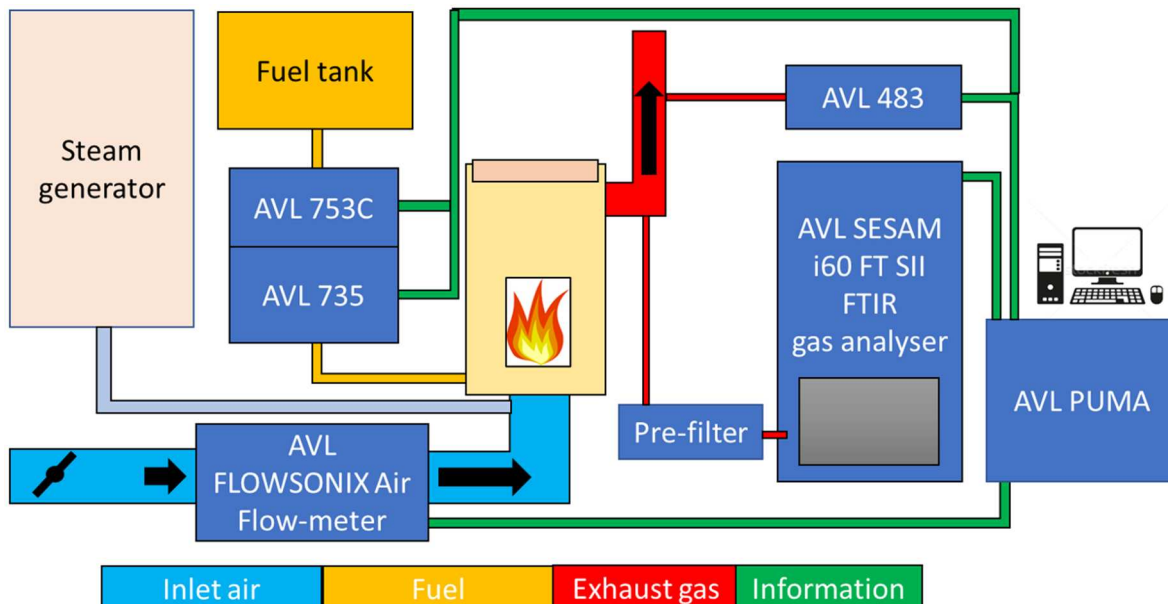


**Figure 2.** Schematic diagram of the experimental setup.

In order to comprehensively analyze the combustion process, a meticulous examination of both the heat distribution within the combustion and the temperature conditions of the combustion chamber was conducted. This investigation was facilitated through the utilization of a FLIR thermal camera, which enabled precise measurements at various points throughout the combustion chamber. The introduction of steam into the combustion chamber was orchestrated by an industrial steam generator, the detailed specifications of which can be found in Table 1. This steam injection process was strategically implemented directly in front of the air inlets, a crucial placement that played a pivotal role in influencing the combustion dynamics. The FLIR thermal camera served as an invaluable tool in capturing real-time data, allowing for an in-depth analysis of the heat distribution patterns during the combustion process. This comprehensive approach not only shed light on the overall efficiency of the combustion but also provided crucial insights into the interplay between steam injection and combustion dynamics within the chamber. The industrial steam generator, as outlined in Table 1, played a central role in regulating the steam injection parameters, ensuring a controlled and precisely managed introduction of steam into the combustion chamber. The synchronized interaction of these components created an environment conducive to a thorough understanding of the combustion behavior and its implications for temperature distribution within the system.

**Table 1.** Technical specification of the Humapress HV6 steam generator.

Maximum steam capacity	6 kg/h
Working pressure	3 bar
Water inlet pressure	4 bar
Boiler capacity	15l
Maximum steam pressure	6 bar
Steam temperature	354 °C
Feed water temperature	20°C
Warm-up time	15 min
Heating power	5 kW
Supply voltage	380V

## 2. Exhaust gas and particulate matter measurement method

The type of equipment used during the measurements is AVL SESAM i60 FT SII, it is a Fourier transform infrared (FTIR) spectrometer. Its measurement principle is based on absorption and reflection. A gas scanned with broad-spectrum infrared light absorbs light rays of certain frequencies and transmits others. The frequency of the absorbed light is the same as the natural frequency of the vibrational modes of the gas molecules, or the harmonics of these frequencies. The ratio of the absorbed light is the same as the concentration ratio of the gas being tested. So the spectrum of the passing absorbed frequency gives the type of gas, and the amount of absorbed light gives the concentration of the gas being tested. [8] Figure 3 schematically illustrates how the infrared light is introduced through a modulator into a cuvette in which the gas to be analysed is flowed. The modulator modulates the light, so it splits it into different wavelengths, and when the light passes through the cuvette, the detector detects the amount of light passing through. From the sensed signal, the electronics infers the degree of absorption, which it converts into the concentration of the analysed gases using Fourier transformation.

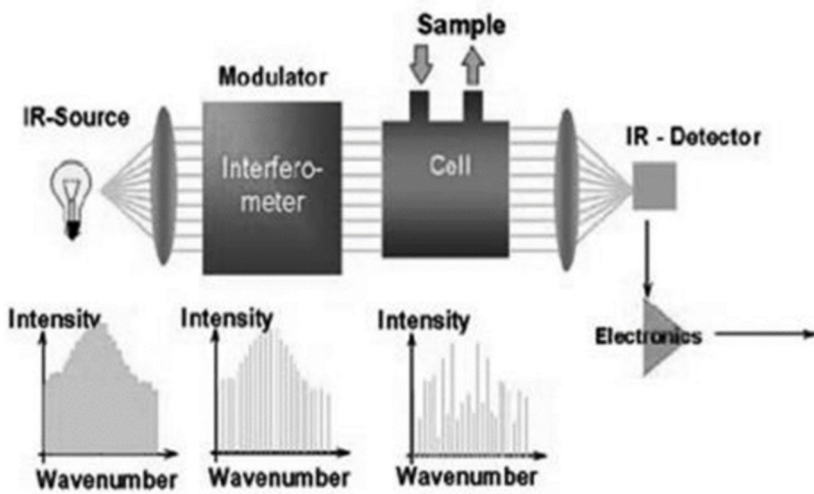


**Figure 3.** AVL FTIR schematic diagram [9].

The AVL Micro Soot Sensor (AVL483) is a sophisticated measuring device employed for the quantification of soot concentration. Operating on the photoacoustic principle, this device utilizes a unique method to assess the concentration of emitted soot. The underlying measurement principle hinges on the distinctive optical properties of soot particles; being black and inherently dark in color, they exhibit a high absorption capacity for light. This absorption phenomenon is vividly depicted in Figure 3. In practical terms, the measuring process involves modulating the measuring light, which is then directed towards the soot particles within the exhaust gas to be analyzed. Due to their dark nature, the soot particles readily absorb the modulated measuring light. This absorption results in the heating of the sample gas, a crucial step in the measurement process [10]. To carry out the measurement, the AVL Micro Soot Sensor extracts a sample from the exhaust gas under examination. This sample is then subjected to illumination, and the ensuing absorption of measuring light facilitates the heating of the sample gas. The device's capacity to effectively capture and analyze the soot concentration in this manner underscores its precision and reliability in environmental and combustion studies.

The process of measuring soot concentration involves the dynamic response of the sample gas in the measuring chamber to changes in temperature and soot particle concentration. Upon heating, the sample gas undergoes expansion, while a reduction in soot particles leads to contraction. This contraction is a consequence of reduced light absorption by fewer soot particles, causing a sudden cooling of the sample gas within the resonant cell, as depicted in Figure 4. The expansion and contraction events generate a discernible sound wave, akin to an acoustic signal, which can be easily captured by a microphone and subsequently transmitted to the control unit for analysis. One notable advantage of this instrument is its ability to directly measure soot concentration without succumbing to cross-sensitivity issues with other components present in the exhaust gas. This specificity is crucial for accurate assessments of soot levels. Additionally, the instrument is proficient in conducting raw exhaust gas measurements, a capability achieved through the ingenious application of thermophoretic loss compensation (TLC). The engineers ingeniously implemented TLC to address challenges arising from thermophoretic deposits at the exhaust gas sampling location. These deposits could lead to a shortage of soot particles in the measured sample. By compensating for this deficiency, TLC ensures that the measured quantity of soot particles is appropriately adjusted to account for any discrepancies introduced by thermophoretic deposits [11]. This feature enhances the instrument's precision and reliability, making it a valuable tool for exhaust gas analysis in various applications.

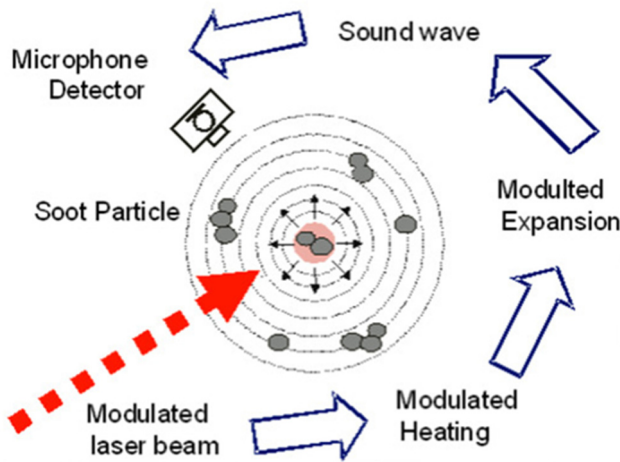


**Figure 4.** Schematic diagram of photoacoustic principle [9].

### 3. Measurement points

The measurements were made at twelve points, so that for three types of fuel flow values (0.3; 0.6; 1 kg/h) four types of air flow values (10; 40; 70; 100 %) were set. The measurement results are presented for a fuel consumption value of 1 kg/h.

#### 3.1. Soot emission

Furthermore, the impact of water vapor on  $\text{NO}_x$  concentration was also investigated, as highlighted in previous studies [12]. The findings revealed a positive influence on both soot and  $\text{NO}_x$  levels. The initial analysis focused on the evolution of soot emissions, with results presented in the first table. Notably, the measurements proceeded from right to left in the diagram, representing a transition from higher to lower throttle positions. The variations in stoichiometry across different working points contributed to distinct values in soot emissions. In the case of diesel fuel, a noteworthy reduction of approximately half in soot emissions was observed at the measured points, underscoring the effectiveness of water vapor. Interestingly, when considering the TPO+Heating oil mixture, a particularly favorable outcome emerged, showcasing a drastic reduction in soot emissions across all measured points. Figure 5 supplements these findings by illustrating the soot concentration for each fuel mixture at various stoichiometric ratios. This visual representation offers a comprehensive view of how different fuel mixtures, in conjunction with varying stoichiometric conditions, influence soot emissions. The observed trends further emphasize the potential of water vapor in mitigating soot concentrations, especially when combined with specific fuel blends.

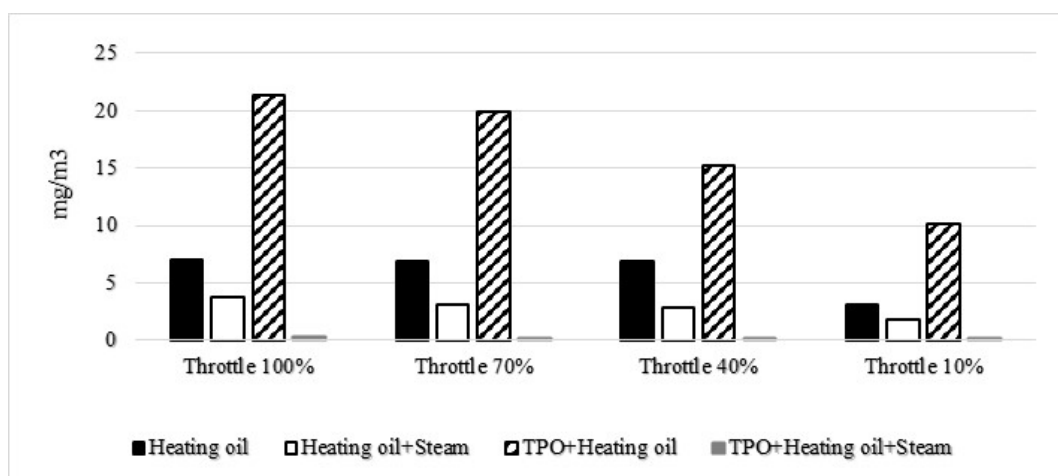


**Figure 5.** evolution of soot emission in the examined measurement point.

### 3.2. $\text{NO}_x$ emission

In the realm of  $\text{NO}_x$  emissions, a parallel pattern emerged akin to the observed trend with carbon black. The introduction of water vapor exhibited a noteworthy reduction in  $\text{NO}_x$  levels for both diesel and diesel TPO blends. These findings align with the outcomes documented in studies focusing on water vapor injections within internal combustion engines [13], thereby substantiating the empirical evidence garnered during our measurements. The mechanism behind the reduction in  $\text{NO}_x$  emissions lies predominantly in the heat-absorbing attributes of water vapor. Upon injection, water vapor plays a pivotal role in extracting heat from the combustion process, consequently mitigating the flame temperature. This pivotal factor is underscored by the temperature distribution profiles depicted in Figure 6. A visual examination of the combustion chamber reveals a distinct disparity between configurations without water vapor injection (left) and those with water vapor injection (right) at the Figure 7. The non-uniform heat distribution in the combustion chamber without water vapor injection underscores the intricacies of combustion by evaporation. This process, while essential for energy release, introduces challenges from an emissions standpoint. The uneven distribution of heat can contribute to suboptimal combustion conditions, leading to heightened emissions, particularly  $\text{NO}_x$ . Consequently, the incorporation of water vapor emerges not only as a strategy for temperature moderation but also as a means to foster a more uniform and controlled combustion environment, thereby contributing to the overall reduction of harmful emissions.

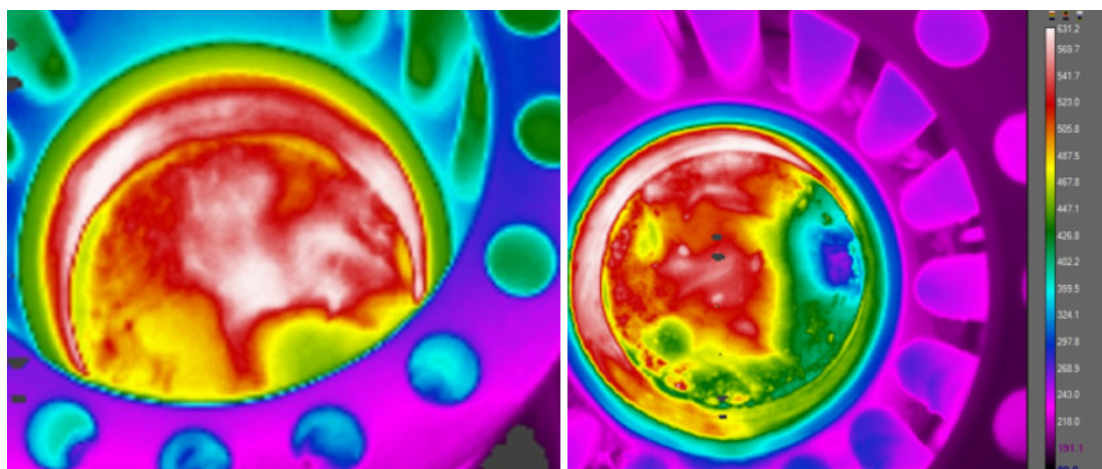


**Figure 6.** Temperature distribution in the combustion chamber for a TPO+Heating oil blend at 100% throttle position with a fuel consumption of 1kg/h.

The evolution of the  $\text{NO}_x$  concentration at the measurement points is shown in the Figure 6.

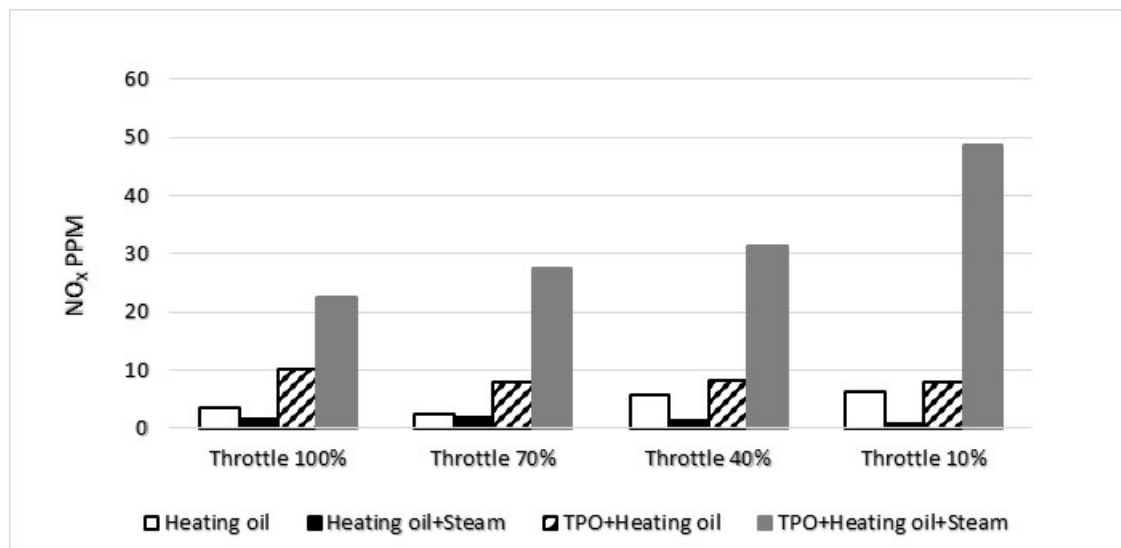


**Figure 7.** evolution of NO<sub>x</sub> in the examined measurement point.

### 3.3. CO<sub>2</sub> emission

Furthermore, the elevated concentration of carbon dioxide in the TPO+Heating oil mixture with water vapor can be attributed to the heightened temperature during combustion. The combustion process of the TPO and Heating oil blend generates increased heat, leading to more significant production of carbon dioxide. Additionally, the uneven distribution of the mixture further contributes to this phenomenon. The inhomogeneous mixture distribution results in varying combustion rates across different regions, influencing the overall carbon dioxide output. In Figure 8, the representation of CO<sub>2</sub> concentrations for each fuel mixture at different stoichiometric ratios provides a visual depiction of the observed trends. The varying stoichiometric ratios highlight the impact of the air-to-fuel ratio on carbon dioxide emissions, emphasizing the importance of understanding and optimizing combustion conditions for environmental considerations.

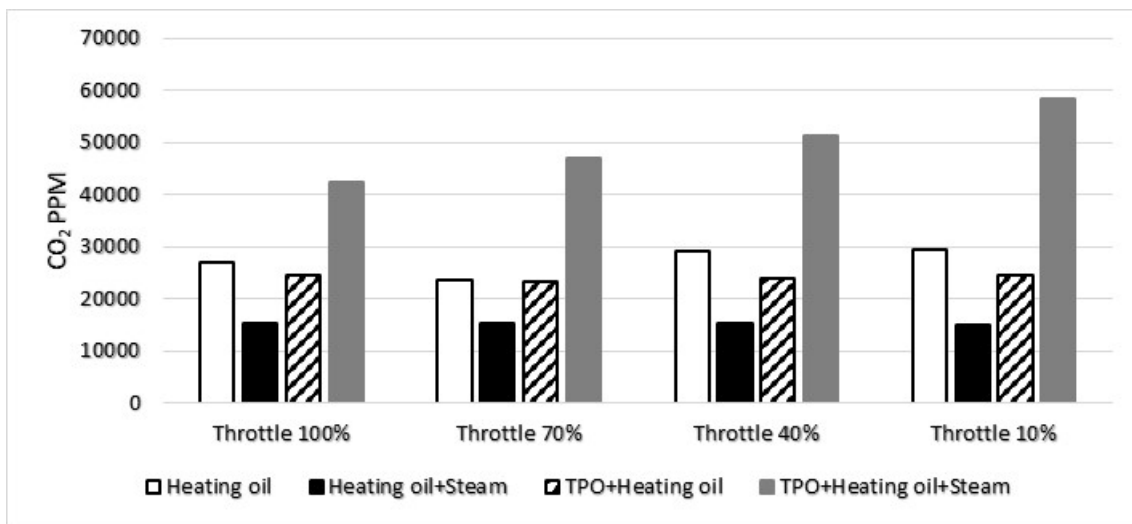


**Figure 8.** CO<sub>2</sub> evolution in the examined measurement point.

### 3.4. CO emission

The addition of water vapor resulted in a significant reduction in carbon monoxide (CO) concentration across all measured operating points. Notably, the extent of this decrease was found to be closely tied to the stoichiometric ratio. The stoichiometric ratio plays a pivotal role in determining the magnitude of carbon monoxide concentration in the observed scenarios. In instances where there is an excess of air, the CO concentration in the flue gas is influenced by both the inhomogeneous mixture distribution and the composition of the mixture [14]. This implies that variations in the distribution of the mixture and its overall composition significantly impact the levels of carbon monoxide present in the flue gas. For a more comprehensive understanding, Figure 9 illustrates the carbon monoxide concentration for each fuel mixture across different stoichiometric ratios. This graphical representation provides a visual insight into how changes in the stoichiometric ratio affect the concentration of carbon monoxide, highlighting the dynamic nature of this relationship in the presence of water vapor. These findings underscore the importance of considering both the stoichiometric ratio and mixture characteristics when analyzing and optimizing combustion processes to minimize carbon monoxide emissions.

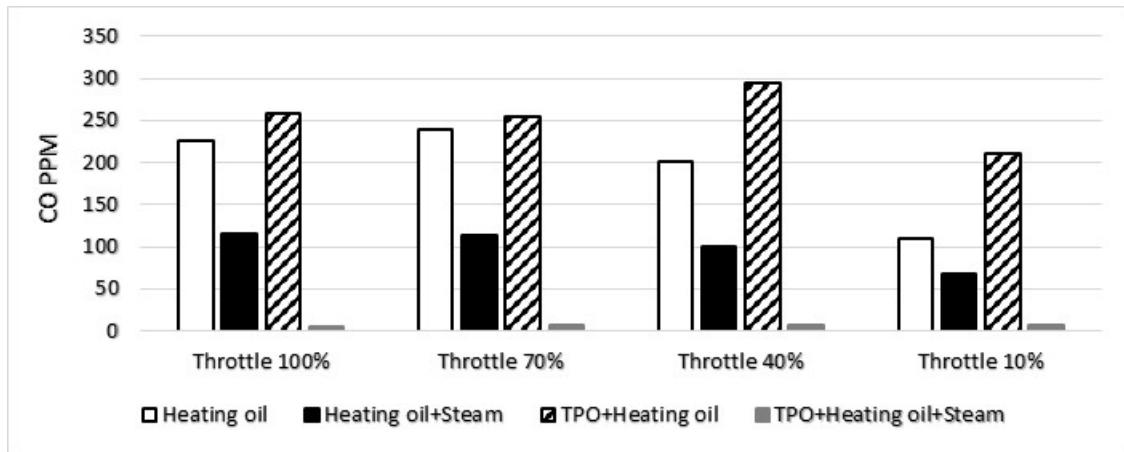


**Figure 9.** evolution of CO emission in the examined measurement point.

### 3.5. Water concentration

At the measurement point where diesel was assessed, the concentration of water was negligible and could not be quantified. Conversely, when examining the TPO combined with heating oil, the presence of water became evident. This is attributed to the inherently higher water content in TPO compared to heating oil. The discernible water content in the TPO+heating oil mixture is graphically represented in Figure 10, highlighting the contrast in water concentrations between the two fuel compositions at the respective measurement points.

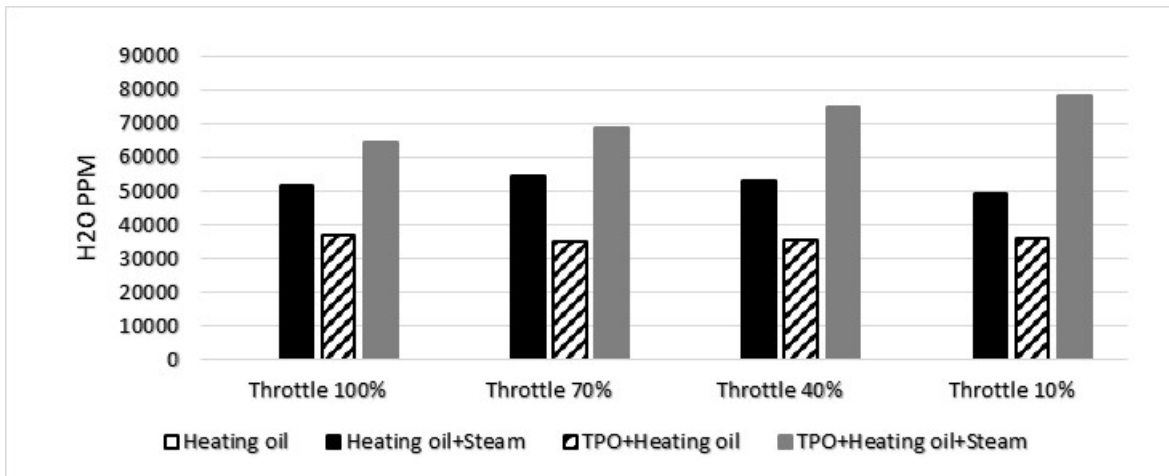


**Figure 10.** Water concentration in the examined measurement point.

## 4. Conclusion

In this research, the profound impact of water vapor on combustion processes has come to light. Scientific understanding has established that water molecules can undergo separation at elevated temperatures, specifically within the range of 1000-1650°C. This thermal process results in the generation of hydrogen and hydroxyl, which subsequently transform into water vapor through thermal decomposition. This decomposition can be orchestrated within a combustion device, effectively occurring in the combustion chamber. The high-temperature environment of the combustion chamber triggers the decomposition of water vapor, giving rise to active hydroxyl and hydrogen, acting as focal points that expedite the breakdown of hydrocarbons. This acceleration, in turn, enhances the combustion rate within the chamber. The catalytic influence of water vapor on combustion becomes evident as hydroxyl and formed hydrogen molecules undergo oxidation,

producing water and hydrogen atoms. Notably, atomic-level hydrogen further amplifies the generation of hydroxyl, perpetuating the cycle until equilibrium is reached concerning temperature, fuel quantity, and water vapor concentration.

Remarkably, water vapor exhibits a catalytic role that practically eliminates gas-phase soot formation. However, caution is warranted, as an excessive concentration of water vapor in the combustion chamber can prove detrimental. The substantial volume of water vapor serves to excessively cool the combustion chamber and the fuel-air mixture, leading to delayed ignition and a protracted combustion process. Additionally, an overabundance of introduced steam may significantly elevate the production of carbon monoxide (CO) during combustion, owing to supercooling effects.

Furthermore, water vapor exerts a nuanced influence on combustion emissions by marginally lowering the flame combustion temperature. This reduction, while beneficial for mitigating thermal nitrogen oxides (NO<sub>x</sub>) production, underscores the delicate balance required in managing water vapor concentrations to optimize combustion efficiency and minimize undesirable side effects. Consequently, understanding and controlling the presence of water vapor within the combustion process emerge as critical considerations for achieving optimal performance and emission profiles.

## Nomenclature

AVL	Anstalt für Verbrennungskraftmaschinen List
TPO	Tire Pyrolysis Oil
H <sub>2</sub> O	Just Add Water
PM	Particulate Matter
NO	Nitrogen Oxides
CO	Carbone Monoxide
CO <sub>2</sub>	Carbon Dioxide
HC	Hydrogen Carbon
FTIR	Fourier Transform Infrared Spectroscopy
TLC	Thermophoretic loss compensation

## References

1. Rodríguez-Fernández, L., Fernández Carvajal, A. B., & Ruiz-Gómez, L. M. (2020). Evolution of European Union's energy security in gas supply during Russia–Ukraine gas crises (2006–2009). *Energy Strategy Reviews*, 30, 100518. doi:10.1016/j.esr.2020.100518
2. Von Homeyer, I., Oberthür, S., & Jordan, A. J. (2021). EU climate and energy governance in times of crisis: towards a new agenda. *Journal of European Public Policy*, 28(7), 959–979. doi:10.1080/13501763.2021.1918221
3. Jirušek, M. (2020). The attitude of the Visegrad Group Countries towards Russian Infrastructural Projects in the gas sector. *Energy Policy*, 139, 111340. doi:10.1016/j.enpol.2020.111340
4. Ederington, L. H., Fernando, C. S., Hoelscher, S., Lee, T. K., & Linn, S. C. (2018). A Review of the Evidence on the Relation Between Crude Oil Prices and Petroleum Product Prices. *SSRN Electronic Journal*. doi:10.2139/ssrn.3249045
5. ARMAS, O., BALLESTEROS, R., MARTOS, F., & AGUDELO, J. (2005). Characterization of light duty Diesel engine pollutant emissions using water-emulsified fuel. *Fuel*, 84(7-8), 1011–1018. doi:10.1016/j.fuel.2004.11.015
6. Kökkünlük, G., Gonca, G., Ayhan, V., Cesur, İ., & Parlak, A. (2013). Theoretical and experimental investigation of diesel engine with steam injection system on performance and emission parameters. *Applied Thermal Engineering*, 54(1), 161–170. doi:10.1016/j.applthermaleng.2013.
7. 04/02008 Diesel engine performance and emission characteristics using the three-phase emulsions as fuel. (2004). *Fuel and Energy Abstracts*, 45(4), 277. doi:10.1016/s0140-6701(04)94595
8. Bak, J., & Clausen, S. (2001). FTIR emission spectroscopy methods and procedures for real time quantitative gas analysis in industrial environments. *Measurement Science and Technology*, 13(2), 150–156. doi:10.1088/0957-0233/13/2/302
9. I. P. Kondor, M. Zöldy, D. Mihály: „Experimental Investigation on the Performance and Emission Characteristic of Compression Ignition Engine Using Waste Based Tire Pyrolysis Fuel and Diesel Fuel Blends,” *Energies*, 2021. <https://doi.org/10.3390/en14237903>

10. Gonca, G., Sahin, B., Parlak, A., Ust, Y., Ayhan, V., Cesur, İ., & Boru, B. (2014). The effects of steam injection on the performance and emission parameters of a Miller cycle diesel engine. *Energy*, 78, 266–275. doi:10.1016/j.energy.2014.10.002
11. Grob, B., Schmid, J., Ivleva, N. P., & Niessner, R. (2012). Conductivity for Soot Sensing: Possibilities and Limitations. *Analytical Chemistry*, 84(8), 3586–3592. doi:10.1021/ac203152z
12. Zhang, Z., Fuehrhapter, R., Waschl, H., & Del Re, L. (2016). Calibration and Performance of a Novel In-situ Soot Sensor for Production Engines. *Procedia Engineering*, 168, 43–46. doi:10.1016/j.proeng.2016.11.135
13. O. Armas, R. Ballesteros, F.J. Martos, J.R. Agudelo, Characterization of light duty diesel engine pollutant emissions using wateremulsified fuel, *Fuel* 84 (2005) 1011e1018
14. Hadia, F., Wadhah, S., Ammar, H., & Ahmed, O. (2017). Investigation of combined effects of compression ratio and steam injection on performance, combustion and emissions characteristics of HCCI engine. *Case Studies in Thermal Engineering*, 10, 262–271. doi:10.1016/j.csite.2017.07.005
15. Xue, J., Grift, T. E., & Hansen, A. C. (2011). Effect of biodiesel on engine performances and emissions. *Renewable and Sustainable Energy Reviews*, 15(2), 1098–1116. doi:10.1016/j.rser.2010.11.016

**Disclaimer/Publisher's Note:** The statements, opinions and data contained in all publications are solely those of the individual author(s) and contributor(s) and not of MDPI and/or the editor(s). MDPI and/or the editor(s) disclaim responsibility for any injury to people or property resulting from any ideas, methods, instructions or products referred to in the content.